analytical chemistry

ARTICLE

pubs.acs.org/ac

Carbohydrate-Based Label-Free Detection of *Escherichia coli* ORN 178 Using Electrochemical Impedance Spectroscopy

Xuefei Guo, Ashish Kulkarni, Amos Doepke, H. Brian Halsall, Suri Iyer,* and William R. Heineman*

Department of Chemistry, University of Cincinnati, Cincinnati, Ohio 45221-0172, United States

Supporting Information

ABSTRACT: A label-free biosensor for *Escherichia coli* (*E. coli*) ORN 178 based on faradaic electrochemical impedance spectroscopy (EIS) was developed. α-Mannoside or β-galactoside was immobilized on a gold disk electrode using a self-assembled monolayer (SAM) via a spacer terminated in a thiol functionality. Impedance measurements (Nyquist plot) showed shifts due to the binding of *E. coli* ORN 178, which is specific for α-mannoside. No significant change in impedance was observed for *E. coli* ORN 208, which does not bind to α-mannoside. With increasing concentrations of *E. coli* ORN 178, electron-transfer resistance (R_{et}) increases before the sensor is saturated. After the Nyquist plot of *E. coli*/mixed SAM/gold electrode was modeled, a linear relationship between normalized R_{et} and the logarithmic value of *E. coli* concentrations was found in a range of bacterial concentration from 10^2 to 10^3 CFU/mL. The combination of robust carbohydrate ligands with EIS provides a label-free, sensitive, specific, user-friendly, robust, and portable biosensing system that could potentially be used in a point-of-care or continuous environmental monitoring setting.

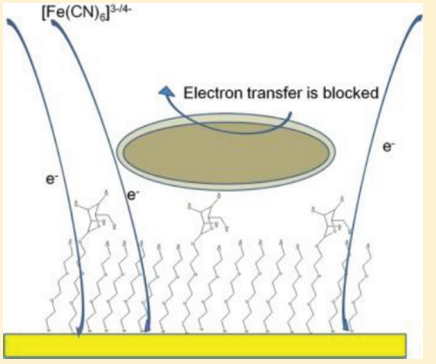

Foodborne diseases have become a cause for concern with outbreaks and food recalls being increasingly commonplace.[1] The Centers for Disease Control (CDC) estimates that 1 in 6 (~48 million) people will get infected annually in the US per annum, and approximately 125 000 people will be hospitalized and 3000 cases will result in untimely death.[2] *E. coli* O157:H7 is one such pathogen that can cause severe disease especially in immune-compromised people and is listed as one of the top five pathogens that result in hospitalization by the CDC. While infection by this bacterium was generally related to beef or uncooked meat contamination in the past, this is no longer the case as more and more incidences have been linked to nonmeat products such as spinach, presumably due to manure runoff, and cookie dough, presumably due to cross-contamination related to processing.[3] Beyond the health and psychosocial impacts of a suspected outbreak, the economic impact can be devastating. In a particular case, the Topps meat processing company, which had over 100 million dollars in assets, had to declare bankruptcy because they were forced to recall 21.7 million pounds of ground beef that was contaminated with *E. coli* O157:H7.[4,5] A different outcome for this company could have been achieved, if "realtime" biosensors had been available at different locations in the food processing and distribution network to catch the problem earlier.

Rapid and sensitive detection and identification of infectious agents are extremely important to prevent catastrophic outbreaks before public consumption. The effective early detection of pathogenic bacteria is dependent on a number of challenging criteria.[6] Analysis time and sensitivity are among the most important factors when evaluating the usefulness of a point-of-care test kit. High selectivity is also required, because low numbers of pathogenic bacteria are often present in a complex medium with many other organisms. Traditional methods such as culture tests for detecting bacteria involve a number of steps and trained personnel. The results from these gold standard culture tests usually take 24−48 h before they are available, making outbreak situations difficult to prevent.

Other point-of-care detection systems include enzyme-linked immunosorbent assay (ELISA),[7] real time polymerase chain reaction (PCR),[8] quartz crystal microbalance resonators (QCM),[9,10] bioconjugated nanoparticles,[11,12] etc. Nucleic acid probe-based techniques require expensive equipment and trained personnel.[13] ELISA exploits antibodies as molecular recognition elements due to their highly specific binding with targets. However, most antibodies have inherent disadvantages because they are expensive to produce and lack the stability required for continuous environmental monitoring.[13] Tailored carbohydrates are increasingly being considered as alternative recognition molecules because of their unique recognition capabilities, small size, and stability under a variety of conditions.[14] Carbohydrates have been coupled to various transducers to detect analytes that range from infectious agents to diseased cells.[15,16] As low as 10^5 bacteria were detected using glyco-dendronized polylysine.[17] Carbohydrate-functionalized quantum dots were used to detect bacteria in cell suspensions containing as few as 10^4 *E. coli*/mL.[18] Magnetic glyco-nanoparticles could reliably detect 10^4 cells/mL.[19] We have been involved in the development of synthetic glycans

Received: September 13, 2011
Accepted: October 28, 2011
Published: October 28, 2011

Scheme 1. Scheme for Detecting *E. coli* by Increasing Electron-Transfer Resistance (R_{et}) through Blocking Bacteria Captured by Sensor Consisting of Mixed SAM with Carbohydrate Binding Ligand

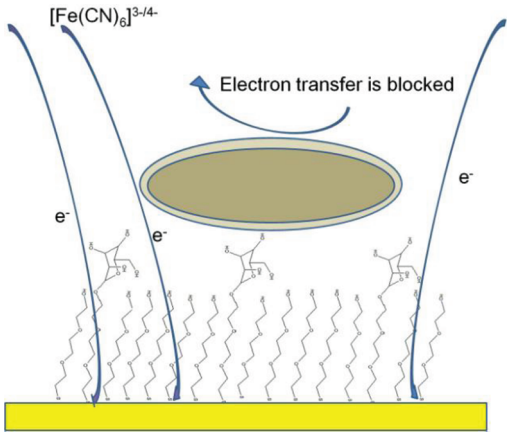

as high affinity receptors for capturing a number of infectious agents including botulinum, shiga and pertussis toxins, influenza viruses, and *E. coli*.[20,21] In this work, we detect bacteria by electrochemical impedance spectroscopy (EIS) after capturing with synthetic glycans and have achieved a lower detection limit of 10^2 CFU/mL.

EIS is a powerful way to analyze the complex electrical resistance of a system and is sensitive to surface phenomena. EIS has been used extensively in a variety of formats, such as elucidating corrosion mechanisms.[22] More recently, this method has attracted considerable interest in biosensors because minute changes in analyte binding to a biosensor surface can be easily and rapidly detected.[23,24] Additionally, EIS is also a valuable and effective tool to characterize surface modifications and detect biorecognition processes.

Impedance biosensors measure the electrical impedance of an interface in AC steady state with constant DC bias conditions. Generally, there are two categories of impedance measurements: nonfaradaic impedance performed in the absence of any redox probe, and faradaic impedance performed in the presence of a redox probe. The most promising applications of electrical biosensors are situations where low cost, portability, and speed of analysis are crucial. One of the advantages of EIS is the small-amplitude perturbation from steady state, which makes it a nondestructive technique. Furthermore, EIS can determine the presence of biomolecules without the need of an additional label. EIS has been employed for label-free biosensors for antibody and ssDNA[25] and as a transducer for detecting bacteria using antibody[26] and using lectin[27,28] or signal amplification such as precipitation.[29]

In this work, we combined the recognition properties of carbohydrates and EIS to develop a biosensor with a transducer mechanism to detect *E. coli* ORN178, which, in this study, is a surrogate to the more pathogenic *E. coli* O157:H7, as depicted in Scheme 1. Immobilizing biological receptors on the biosensor surface is an important factor affecting the sensitivity and specificity of detection. It is crucial that the probe molecule be attached to the sensor surface in a way that maintains the specificity and activity of the probe while inhibiting nonspecific binding. Self-assembled monolayers (SAMs) have been exploited extensively to provide model surfaces for potential applications[30] in chemical sensing, biosensing, biomimetics, and biocompatibility since 1983.[31,32] The design flexibility of the SAM technique allows various biological macromolecules and living organisms to be immobilized. Alkanethiolate SAMs are widely used on gold surfaces among various kinds of SAMs. For our study, we used α-mannoside and a spacer alcohol thiol to develop a stable SAM on a gold electrode. We demonstrate that rapid detection of bacteria can be achieved using this sensor.

EXPERIMENTAL SECTION

Chemicals and Materials. All chemical reagents were of analytical grade, used as supplied without further purification unless indicated. $NaH_2PO_4 \cdot 2H_2O$, Na_2HPO_4, H_2SO_4, NaOH, H_2O_2, $K_3Fe(CN)_6$, and LB Broth Miller were from Fisher Scientific. $K_4Fe(CN)_6 \cdot 3H_2O$ was obtained from Matheson Coleman & Bell. Deionized water was prepared by a NANOpure system. Anhydrous ethanol was from Pharmoco AAPER, and Syringe Driven Filters were from Millipore. Agar was from Becton Dickinson & Company Sparks. Gold disk electrodes were obtained from BASi. Alumina powders (0.3, 0.1, and 0.05 μm) were purchased from Buehler. EIS was performed on a Gamry Reference 600. SEM images of electrodes were obtained with an environmental scanning electron microscope (ESEM, XL30, Philips). The synthesis of α-mannoside and β-galactoside (compound **3** and **6**) are described in the Supporting Information (SI). The synthesis of spacer ligand, thiolated triethylene glycol (9-mercapto-3,6-dioxaoctan-1-ol), was performed as described previously.[33]

Pretreatment of Electrode. Gold disk electrodes (diameter = 0.16 cm) were pretreated as reported.[34] First, the bare gold disk was polished with 0.3, 0.1, and 0.05 μm alumina powders. Then the electrode was rinsed with DI H_2O and ethanol, and sonicated for 3 min. The polished gold disk was exposed to a freshly prepared piranha solution (Caution!) for 5 min and rinsed intensively with DI H_2O and ethanol. The cleaned electrode was dried under N_2 flow.

Formation of SAM. After drying, the gold disk electrode was immersed immediately into a mixed aqueous thiol solution for at least 12 h. The SAM was generated using various mixtures of a thiol-terminated α-mannoside (compound **3** in SI) and a thiol-terminated oligoethylene glycol "spacer" molecule. The thiols anchored the molecule on the Au surface. The spacer molecule, consisting of ethylene glycol ($[OCH_2CH_2]_3OH$) and SH groups, was used because it is well-known that oligoethylene glycols inhibit nonspecific binding.[32] This simple setup provides a well-defined surface chemistry and highly stable SAM. The mixed SAMs were stabilized by immersing in PBS (pH 7.2) and were monitored by EIS.

EIS Experiments. EIS was run in a single-compartment three-electrode glass cell containing 15 mL of PBS (pH 7.2) and 0.1 M $K_3Fe(CN)_6/K_4Fe(CN)_6$ (1:1 mixture). Platinum wire and Ag/AgCl electrode (filled with 3 M KCl) were used as counter electrode and reference electrode, respectively. Impedance measurements were measured at an open circuit potential to the Ag/AgCl electrode. An alternating potential with a 5 mV amplitude was applied in the frequency range from 0.05 Hz to 1000 kHz. Echem Analyst from Gamry was used to analyze the impedance spectra. All electrochemical measurements were performed in a Faraday cage.

Bacterial Strain and Culture. The two *E. coli* strains used in this study, ORN 178 and ORN 208, were kindly provided by

dx.doi.org/10.1021/ac202419u |*Anal. Chem.* 2012, 84, 241–246

Scheme 2. A Typical Nyquist Plot (Z_{Im} vs Z_{re}) of (a) a Faradaic Impedance Spectrum and (b) Equivalent Circuit of Faradaic Electrochemical Impedance Measurement

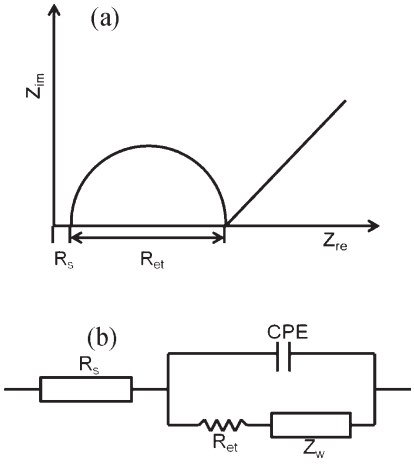

Professor Orndorff.[35] The bacteria were cultured in LB broth at 37 °C for 18 h. The number of viable cells was determined by conventional colony counting on an agar plate. The crude cultured cell sample was diluted with filtered PBS to desired concentrations and stored in the refrigerator.

RESULTS AND DISCUSSION

Characterization of α-Mannoside SAM. Preparing a film on an electrically conductive surface that could capture *E. coli* with the mannose ligand and that had adequate stability and reproducibility was a critical step in developing the sensor. The strategy was to use SAM chemistry to immobilize the mannose ligand on a gold electrode via a thiol linkage. Because the mannose ligand is somewhat bulky, a short-chain spacer thiol was used to adjust the density of mannose ligands on the surface to optimize stability and capture efficiency.

$[Fe(CN)_6]^{3-/4-}$ is often used as a redox probe when characterizing a SAM because the electron transfer of $[Fe(CN)_6]^{3-/4-}$ is impeded by the formation of a highly organized monolayer on the conductive electrode surface.[36,37] Thus, the quality and stability of a SAM, an electrical barrier, can be determined by the electron-transfer resistance of the redox probe $[Fe(CN)_6]^{3-/4-}$, which can be measured using EIS. EIS combines the analysis of the resistive and capacitive properties at the surface of the electrode, based on the perturbation of a system at equilibrium using a small sinusoidal excitation signal.

A Nyquist diagram (Z_{im} vs Z_{re}) of the electrochemical impedance spectrum is an effective way to measure the electron-transfer resistance, as in Scheme 2a. A typical shape of a faradaic impedance spectrum represented in a Nyquist plot includes a semicircular region lying on the Z_{re} axis followed by a straight line with a slope of 45°. The linear part is at the lower frequencies and represents the diffusion-limited electron-transfer process. At higher frequencies, a semicircle is formed due to the electron-transfer processes. The impedance spectrum of a clean gold electrode could include only the linear part because of very fast electron-transfer. A very slow electron-transfer step results in a big semicircle, which is not accompanied by a straight line. Usually, the spectra consist of both the semicircle and linear part. The diameter of the semicircle equals the electron-transfer resistance (R_{et}) of the redox probe. The obtained spectra can be modeled with equivalent circuit models (Scheme 2b), which are helpful for interpreting the electrical properties of the surface of the biosensor.

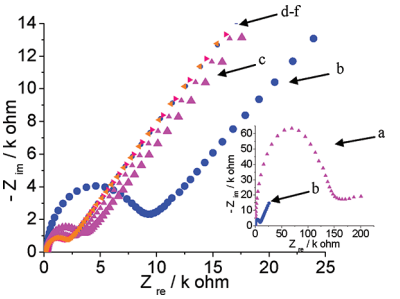

Figure 1. EIS Nyquist diagrams showing stabilization of a SAM of 1:40 α-mannoside:spacer in PBS (pH 7.2) and 0.1 M $K_3[Fe(CN)_6]$/$K_4[Fe(CN)_6]$ (1:1 mixture). a–f are the spectra for 0 min, 2 h, 3 h, 4 h, 5 h, and 2 d.

A thiol-terminated α-mannoside (compound **3** in SI) and a thiol-terminated oligoethylene glycol "spacer" molecule were immobilized on a clean gold electrode by forming a SAM. We first examined the EIS characteristics of the bare gold surface. After polishing and immersing in Piranha solution, all the clean gold disk electrodes produced a nearly linear Nyquist plot without the semicircle, indicating fast electron transfer with $[Fe(CN)_6]^{3-/4-}$. After SAM formation by immobilizing the mixed thiols, semicircles with a diameter of hundreds of kohms were obtained by EIS, which was consistent with the expected blocking of electron transfer of the probe. However, the impedances of different samples of SAM-coated gold were not identical even with the same preparation conditions, electrode, and mixed thiol solution. We attribute this small variability to slight differences in surface states of bare gold from electrode to electrode.[38] The gold electrodes modified with mixed SAMs were then conditioned in phosphate-buffered saline (PBS) before they were used for the detection of *E. coli*. After immersion of a gold electrode coated with a SAM of mixed thiols in PBS, the diameter of the semicircle of the Nyquist plots changed during incubation. Representative results for a 1:40 ratio of α-mannoside:spacer are shown in Figure 1. EIS reveals a significant rearrangement of the SAM occurring during the first 2 h (Figure 1 inset), after which the rearrangement slowed down as equilibrium was approached (Figure 1). Some variability in this conditioning step was observed from electrode to electrode. Electrodes with SAMs of 1:40 ratio of α-mannoside:spacer had different initial impedances, took different time periods (5 h to 2 d) to reach equilibrium, and had different final interfacial R_{et} values (1.6 kΩ to 30 kΩ) as determined from the diameter of semicircles in the Nyquist plots. However, the general trend observed by EIS during the conditioning step was always the same as shown in Figure 1, and these electrodes effectively captured *E. coli*.

As expected, the ratio of α-mannoside to spacer molecule proved critical to the formation of stable SAMs and to their ability to capture *E. coli*. Initially, we failed to develop stable SAMs using a 1:2 mixture of α-mannoside and spacer molecule after incubation, presumably due to steric hindrance caused by the large carbohydrate head groups. These unstable SAMs were also ineffective for capturing *E. coli*. However, decreasing the ratio of α-mannoside:spacer gave substantial improvements.

dx.doi.org/10.1021/ac202419u |*Anal. Chem.* 2012, 84, 241–246

A 1:40 ratio of α-mannoside:spacer achieved good stability after incubation and effectively captured *E. coli* (vide infra).

The stability of SAMs can be influenced by a number of factors, such as light and the condition of the gold surface, which can limit the application of SAMs for biosensors.[39,40] Functional groups of thiols play an important role in ordering SAMs due to the existence of an electrostatic force or hydrogen bonding of adjacent thiols or thiols with solvent molecules.[41] SAM desorption, rearrangement of pinholes, and changes in molecular conformation can also lead to the changes of SAMs in PBS.[30] To minimize the uncertainties for improving reproducibility, we strictly controlled pH, the concentration of $[Fe(CN)_6]^{3-/4-}$, and incubation of the SAMs. All the modified electrodes were incubated in filtered PBS between EIS measurements. Bogomolova reported an increasing diameter of the semicircle in Nyquist plots by repeated measurements.[40] However, the diameter decreased before reaching equilibrium in our case. This may be due to ion permeation into a SAM consisting of 1:40 α-mannoside: spacer.[42]

Detecting *E. coli* by EIS. The ORN 178 strain of *E. coli* expresses wild-type type 1 pili-specific for α-mannoside binding; whereas, the ORN 208 strain expresses abnormal type 1 pili that fails to mediate mannose-specific binding.[35] The binding of ORN 178 to the surface of the sensor results from the recognition element-mannose in the thiol-terminated α-mannoside. The spacer thiol, terminated oligoethylene glycol, can influence the glycan presentation besides blocking nonspecific adsorption. Glycans can adopt several thermodynamically stable conformations, and the ability of a glycan to adopt the conformation needed for receptor recognition can be influenced by adjacent residues that play a limited role in the recognition process. In other words, the spacers can also influence the binding. The density of glycan is also important. While the interactions of pathogens with cell surface carbohydrates are often multivalent, resulting in higher binding avidity compared to monovalent binding, extremely dense packed receptors are not necessary for the binding of *E. coli*.[43] For our system, a 1:40 ratio of the α-mannoside:spacer not only led to the most stable SAM, but also provided the most reliable, reproducible, and significant response to bacteria by sufficient multivalency to capture the bacteria. This implies that an appropriate molecular conformation was achieved for a 1:40 ratio, and that this appropriate molecular conformation may contribute to the stable SAM and capture of bacteria onto the SAM.

After the SAM was stabilized, it showed a reliable response to attaching bacteria. The stabilized sensor was incubated in each prepared *E. coli* solution for 30 min at room temperature. Plots a−j in Figure 2 show that EIS can sense bacteria attaching to the surface of the mannose-modified electrode without signal amplification. The interfacial R_{et} increased with increasing concentrations of *E. coli* ORN 178 cells. Detecting bacteria by impedance lies in the electrical nature of bacterial cells and their electrophysiology. The cell membrane consists of a lipid bilayer and is highly insulated,[44] which can block R_{et} (Scheme 1). With higher concentrations of *E. coli* ORN 178, more bacteria were attached to the electrode surface, more effectively blocking electron transfer and thus leading to a larger diameter of the corresponding semicircle in the Nyquist plot.

Because ORN 208 strain expresses abnormal type 1 pili that fail to mediate mannose-specific binding, it serves as a good control to verify that the EIS response is not due to nonspecific binding to the SAM. The plots with black squares in Figure 2

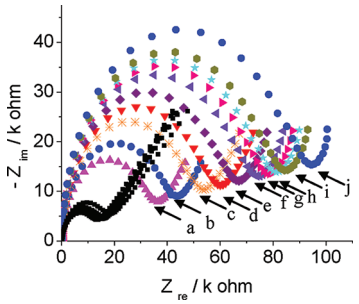

Figure 2. EIS Nyquist diagrams (Z_{im} vs Z_{re}) of a gold disk electrode modified with 1:40 α-mannoside:spacer mixed SAM that correspond to different concentrations of *E. coli* in PBS containing 0.1 M $K_3[Fe(CN)_6]/K_4[Fe(CN)_6]$ (1:1 mixture). a−j are spectra of *E. coli* ORN 178 concentrations of 0, 1.2×10^2, 2.5×10^2, 4.9×10^2, 7.4×10^2, 9.9×10^2, 1.5×10^3, 2.0×10^3, 2.5×10^3, and 1.2×10^4 CFU/mL, respectively. Plots with black squares are controls with *E. coli* ORN 208.

were recorded for *E. coli* ORN 208 as controls. Due to abnormal type 1 pili, α-mannoside failed to bind with ORN 208. Thus, the R_{et} did not increase with higher concentrations of *E. coli* ORN 208. A sensor prepared with the nonbinding ligand β-galactosidase is another control used to verify the sensor's selectivity. EIS spectra showed no response to higher concentrations of *E. coli* ORN 178, which was similar to the control experiments in Figure 2. Thus, the conclusion can be drawn that the sensor with α-mannoside has good selectivity over the bacteria without wild-type 1 pili. Careful selection of recognition elements such as tailored carbohydrates, aptamers, small peptides, or fragments of antibodies,[45,46] etc., would expand applications of this straightforward, portable sensor setup.

The electrochemical impedance data can be simulated with an equivalent model using commercial software, and we used Gamry Echem Analyst to simulate the spectra. A typical equivalent circuit of an electrochemical cell in the presence of a redox probe is presented in Scheme 2b. The equivalent circuit consists of the ohmic resistance of the electrolyte (R_s), the Warburg impedance (Z_w), the constant phase element (CPE), and the R_{et}. Z_w represents the delay arising from diffusion of the electroactive species to the electrode and is appreciable at low frequencies and is affected by convection. The impedance of solid electrodes usually deviates from purely capacitive behavior, so CPE is used instead of a pure capacitance. It has been suggested that surface effects and inhomogeneous current distribution contribute to CPE behavior.[25]

The extracted R_{et} from simulated data was normalized by subtracting R_{et} for blank PBS and dividing by R_{et} at the saturation concentration. The relationship between normalized R_{et} and the *E. coli* concentrations is shown in Figure 3a. R_{et} increased with higher concentration of ORN 178, and the sensor was saturated with bacteria at 2.5×10^3 CFU/mL and higher concentrations. Our results are comparable to and the limit of detection is better than previously reported carbohydrate-based bacterial detection.[17−19] Figure 3b is the enlarged view of the unsaturated part in Figure 3a. A linear relationship between normalized R_{et} and the logarithmic value of *E. coli* concentrations was found in a range of bacterial concentrations from 1.2×10^2 to 2.5×10^3 CFU/mL with a correlation coefficient of 0.98 (Figure 3b). A plot of this type would be a practical calibration curve for the sensor.

***E. coli* Characterization by Scanning Electron Microscope (SEM).** To visualize the capture of bacteria by the α-mannoside-coated

dx.doi.org/10.1021/ac202419u |*Anal. Chem.* 2012, 84, 241–246

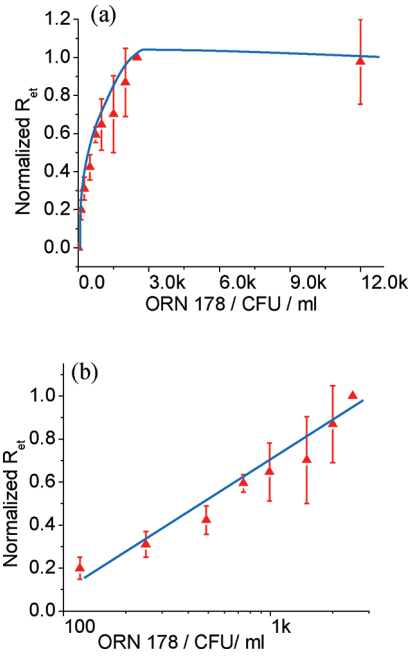

Figure 3. (a) Relationship between normalized R_{et} and *E. coli* ORN 178 concentrations with error bars (n = 3). (b) Linear fitting with a logarithmic abscissa in a range of bacterial concentrations from 120 to 2500 CFU/mL.

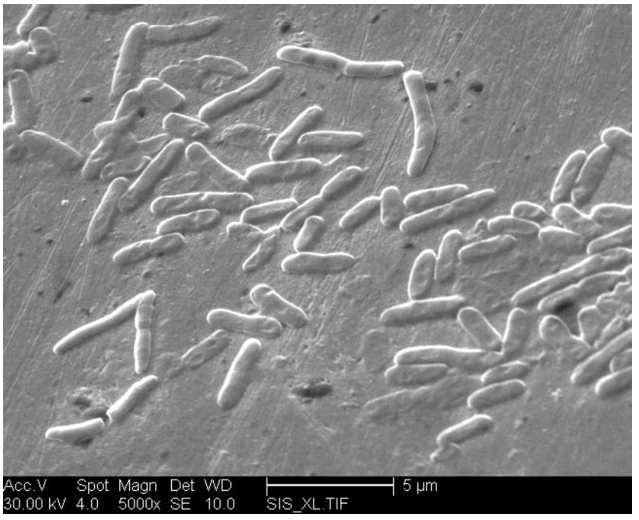

Figure 4. SEM image of the *E. coli* ORN 178 captured by α-mannoside on a gold electrode.

electrode, we used SEM to image *E. coli* on the sensor surface. Briefly, an electrode coated with a SAM of 1:40 α-mannoside:spacer that had both been immersed in *E. coli* ORN 178 was characterized by SEM to confirm that the bacteria remained attached to the sensor after copious rinsing with PBS and DI H_2O and air drying. The SEM shows adherence of many bacteria to the α-mannoside-coated SAM (Figure 4), indicating the strong multivalent interactions between α-mannoside and *E. coli* ORN 178. By comparison, the SEM of a clean, bare gold electrode immersed in the solution of *E. coli* ORN 178 and rinsed showed no bacteria adhering to the bare gold electrode (not shown).

CONCLUSIONS

A rapid, simple, inexpensive, and label-free biosensor that detects bacteria with a combination of the advantage of EIS, functionalization via a SAM, and the selective recognition of carbohydrates has been demonstrated. This detection system has a sensitive response for bacteria in the range of 10^2 to 10^3 CFU/mL. The biosensor can be used as a continuous response sensor, where increasing concentrations of the bacteria will give increasing response until saturation is reached. The method may be expanded readily to detect a wide variety of pathogenic cells by changing the carbohydrate. On the basis of the preliminary results, this system has promise for further development into a portable biosensor.

ASSOCIATED CONTENT

Supporting Information. Additional material as noted in the text. This material is available free of charge via the Internet at http://pubs.acs.org.

AUTHOR INFORMATION

Corresponding Author

*E-mail: suri.iyer@uc.edu (S.I.); heinemwr@uc.edu (W.R.H.).

ACKNOWLEDGMENT

W.R.H. thanks the National Science Foundation (NSF) for generous support (NSF ERC 0812348). S.I. thanks NIAID (U01-AI075498, Alison A. Weiss and S.I.) and NSF (Career CHE-0845005, S.I.) for providing financial support. We thank Necati Kaval (Center for Chemical Sensors & Biosensors, University of Cincinnati) for help with SEM characterization.

REFERENCES

(1) Food safety and foodborne illness. World Health Organization Fact Sheet No. 237, 2007.
(2) Mead, P. S.; Slutsker, L.; Griffin, P. M.; Tauxe, R. V. *Emerg. Infect. Dis.* **1999**, *5* (6), 841–842.
(3) Lashley, F. R. *Expert Rev. Anti.-Infect. Ther.* **2004**, *2* (2), 299–316.
(4) Nugen, S. R.; Baeumner, A. J. *Anal. Bioanal. Chem.* **2008**, *391*, 451–454.
(5) *Nat. Rev. Microbiol.* **2007**, *5*, 836−837.
(6) Ivnitski, D.; Abdel-Hamid, I.; Atanasov, P.; Wilkins, E. *Biosens. Bioelectron.* **1999**, *14* (7), 599–624.
(7) Daly, P.; Collier, T.; Doyle, S. *Lett. Appl. Microbiol.* **2002**, *34* (3), 222–226.
(8) Johnson, R. P.; Durham, R. J.; Johnson, S. T.; Macdonald, L. A.; Jeffrey, S. R.; Butman, B. T. *Appl. Environ. Microb.* **1995**, *61* (1), 386–388.
(9) Otto, K.; Silhavy, T. J. *Proc. Natl. Acad. Sci. U.S.A.* **2002**, *99* (4), 2287–2292.
(10) Shen, Z. H.; Huang, M. C.; Xiao, C. D.; Zhang, Y.; Zeng, X. Q.; Wang, P. G. *Anal. Chem.* **2007**, *79* (6), 2312–2319.
(11) Zhao, X. J.; Hilliard, L. R.; Mechery, S. J.; Wang, Y. P.; Bagwe, R. P.; Jin, S. G.; Tan, W. H. *Proc. Natl. Acad. Sci. U.S.A.* **2004**, *101* (42), 15027–15032.
(12) Carvalho de Souza, A. C.; Halkes, K. M.; Meeldijk, J. D.; Verkleij, A. J.; Vliegenthart, J. F. G.; Kamerling, J. P. *ChemBioChem* **2005**, *6* (5), 828–831.
(13) McAlpine, M. C.; Mannoor, M. S.; Zhang, S. Y.; Link, A. J. *Proc. Natl. Acad. Sci. U.S.A.* **2010**, *107* (45), 19207–19212.
(14) Ngundi, M. M.; Kulagina, N. V.; Anderson, G. P.; Taitt, C. R. *Expert Rev. Proteomics* **2006**, *3* (5), 511–524.
(15) Karlsson, K. A. *Biochem. Soc. Trans.* **1999**, *27* (4), 471–474.

(16) Zhang, X. A.; Teng, Y. Q.; Fu, Y.; Xu, L. L.; Zhang, S. P.; He, B.; Wang, C. G.; Zhang, W. *Anal. Chem.* **2010**, *82* (22), 9455–9460.
(17) Laurino, P.; Kikkeri, R.; Azzouz, N.; Seeberger, P. H. *Nano Lett.* **2011**, *11* (1), 73–78.
(18) Mukhopadhyay, B.; Martins, M. B.; Karamanska, R.; Russell, D. A.; Field, R. A. *Tetrahedron Lett.* **2009**, *50* (8), 886–889.
(19) El-Boubbou, K.; Gruden, C.; Huang, X. *J. Am. Chem. Soc.* **2007**, *129* (44), 13392–13393.
(20) Kale, R. R.; Clancy, C. M.; Vermillion, R. M.; Johnson, E. A.; Iyer, S. S. *Bioorg. Med. Chem. Lett.* **2007**, *17* (9), 2459–2464.
(21) Millen, S. H.; Lewallen, D. M.; Herr, A. B.; Iyer, S. S.; Weiss, A. A. *Biochemistry* **2010**, *49* (28), 5954–5967.
(22) Juttner, K. *Electrochim. Acta* **1990**, *35* (10), 1501–1508.
(23) Pejcic, B.; De Marco, R. *Electrochim. Acta* **2006**, *51* (28), 6217–6229.
(24) Lisdat, F.; Schafer, D. *Anal. Bioanal. Chem.* **2008**, *391* (5), 1555–1567.
(25) Daniels, J. S.; Pourmand, N. *Electroanal.* **2007**, *19* (12), 1239–1257.
(26) Maalouf, R.; Fournier-Wirth, C.; Coste, J.; Chebib, H.; Saikali, Y.; Vittori, O.; Errachid, A.; Cloarec, J. P.; Martelet, C.; Jaffrezic-Renault, N. *Anal. Chem.* **2007**, *79* (13), 4879–4886.
(27) Zhang, D.; Wan, Y.; Hou, B. *Talanta* **2009**, *80* (1), 218–223.
(28) Pingarron, J. M.; Gamella, M.; Campuzano, S.; Parrado, C.; Reviejo, A. J. *Talanta* **2009**, *78* (4−5), 1303–1309.
(29) Ruan, C. M.; Yang, L. J.; Li, Y. B. *Anal. Chem.* **2002**, *74* (18), 4814–4820.
(30) Poirier, G. E. *Chem. Rev.* **1997**, *97* (4), 1117–1127.
(31) Nuzzo, R. G.; Allara, D. L. *J. Am. Chem. Soc.* **1983**, *105* (13), 4481–4483.
(32) Mrksich, M. *Chem. Soc. Rev.* **2000**, *29* (4), 267–273.
(33) Russell, D. A.; Schofield, C. L.; Mukhopadhyay, B.; Hardy, S. M.; McDonnell, M. B.; Field, R. A. *Analyst* **2008**, *133* (5), 626–634.
(34) Damos, F. S.; Luz, R. C. S.; Kubota, L. T. *Langmuir* **2005**, *21* (2), 602–609.
(35) Harris, S. L.; Spears, P. A.; Havell, E. A.; Hamrick, T. S.; Horton, J. R.; Orndorff, P. E. *J. Bacteriol.* **2001**, *183* (13), 4099–4102.
(36) Markovich, I.; Mandler, D. *J. Electroanal. Chem.* **2000**, *484* (2), 194–202.
(37) Boubour, E.; Lennox, R. B. *Langmuir* **2000**, *16* (9), 4222–4228.
(38) Diao, P.; Guo, M.; Tong, R. *J. Electroanal. Chem.* **2001**, *495*, 98–105.
(39) Dijksma, M.; Kamp, B.; Hoogvliet, J. C.; van Bennekom, W. P. *Langmuir* **2000**, *16* (8), 3852–3857.
(40) Bogomolova, A.; Komarova, E.; Reber, K.; Gerasimov, T.; Yavuz, O.; Bhatt, S.; Aldissi, M. *Anal. Chem.* **2009**, *81* (10), 3944–3949.
(41) Li, Z.; Niu, T.; Zhang, Z.; Feng, G.; Bi, S. *Thin Solid Films* **2011**, *519*, 4225–4233.
(42) Bjorefors, F.; Petoral, R. M.; Uvdal, K. *Anal. Chem.* **2007**, *79* (21), 8391–8398.
(43) Kulkarni, A. A.; Weiss, A. A.; Iyer, S. S. *Med. Res. Rev.* **2010**, *30* (2), 327–393.
(44) Pethig, R.; Markx, G. H. *Trends Biotechnol.* **1997**, *15* (10), 426–432.
(45) Tombelli, S.; Minunni, M.; Mascini, M. *Biomol. Eng.* **2007**, *24* (2), 191–200.
(46) Ngundi, M. M.; Kulagina, N. V.; Anderson, G. P.; Taitt, C. R. *Expert Rev. Proteomics* **2006**, *3* (5), 511–24.